J Lipid Atheroscler. 2020 Jan;9(1):110-123
https://doi.org/10.12997/jla.2020.9.1.110
pISSN 2287-2892·eISSN 2288-2561

JLA Journal of Lipid and Atherosclerosis

Review

Check for updates

Quantifications of Lipid Kinetics *In Vivo* Using Stable Isotope Tracer Methodology

Il-Young Kim,[1] **Sanghee Park**,[1] **Jiwoong Jang**,[1] **Robert R. Wolfe**[2]

[1]Department of Molecular Medicine, Lee Gil Ya Cancer and Diabetes Institute, College of Medicine, Gachon University, Incheon, Korea
[2]Department of Geriatrics, Center for Translational Research in Aging & Longevity, Donald W. Reynolds Institute on Aging, University of Arkansas for Medical Sciences, Little Rock, AR, USA

OPEN ACCESS

Received: Nov 5, 2019
Revised: Dec 19, 2019
Accepted: Dec 29, 2019

Correspondence to
Il-Young Kim
Department of Molecular Medicine, Lee Gil Ya Cancer and Diabetes Institute, College of Medicine, Gachon University, 155 Gaetbeol-ro, Yeonsu-gu, Incheon 21999, Korea.
E-mail: iykim@gachon.ac.kr

ORCID iDs
Il-Young Kim
https://orcid.org/0000-0002-6314-2415
Sanghee Park
https://orcid.org/0000-0003-1632-3448
Jiwoong Jang
https://orcid.org/0000-0002-9127-9494
Robert R. Wolfe
http://orcid.org/0000-0003-3425-8889

Funding
Kim IY: Basic Science Research Program through the National Research Foundation of Korea (NRF) funded by the Ministry of Education (2018R1D1A1B07051053); Korea Research Fellowship (KRF) funded by the Ministry of Science and ICT and National Research Foundation of Korea (2019H1D3A1A01071043).

ABSTRACT

Like other bodily materials, lipids such as plasma triacylglycerol, cholesterols, and free fatty acids are in a dynamic state of constant turnover (i.e., synthesis, breakdown, oxidation, and/or conversion to other compounds) as essential processes for achieving dynamic homeostasis in the body. However, dysregulation of lipid turnover can lead to clinical conditions such as obesity, fatty liver disease, and dyslipidemia. Assessment of "snap-shot" information on lipid metabolism (e.g., tissue contents of lipids, abundance of mRNA and protein and/or signaling molecules) are often used in clinical and research settings, and can help to understand one's health and disease status. However, such "snapshots" do not provide critical information on dynamic nature of lipid metabolism, and therefore may miss "true" origin of the dysregulation implicated in related diseases. In this regard, stable isotope tracer methodology can provide the *in vivo* kinetic information of lipid metabolism. Combining with "static" information, knowledge of lipid kinetics can enable the acquisition of in depth understanding of lipid metabolism in relation to various health and disease status. This in turn facilitates the development of effective therapeutic approaches (e.g., exercise, nutrition, and/or drugs). In this review we will discuss 1) the importance of obtaining kinetic information for a better understanding of lipid metabolism, 2) basic principles of stable isotope tracer methodologies that enable exploration of "lipid kinetics" *in vivo*, and 3) quantification of some aspects of lipid kinetics *in vivo* with numerical examples.

Keywords: Lipid metabolism; Substrate turnover, Dyslipidemia; Mass spectrometry

INTRODUCTION

Once thought to be static, lipids in the body turn over at varying rates to achieve overall "dynamic" homeostasis as do other bodily materials.[1] Current understanding of the dynamic nature of lipids in the body is largely attributed to stable isotope tracer-based metabolic research, particularly to the pioneering research by Schoenheimer and his colleagues.[1-3] The lipid pool size in tissues such as plasma, adipose tissue, and liver can change if an imbalance between rates of appearance (R_a) into and disappearance (R_d) from the compartment occurs in normal (e.g., exercise) or pathological processes (e.g., non-alcoholic fatty liver disease, NAFLD) over time. For example, plasma hypertriglyceridemia, an excess of plasma

Conflict of Interest
The authors have no conflicts of interest to declare.

Author Contributions
Conceptualization: Kim IY; Supervision: Kim IY, Wolfe RR; Writing - original draft: Kim IY; Writing - review & editing: Kim IY, Park S, Jang J, Wolfe RR.

triacylglycerol (TAG) concentrations particularly in postprandial state that is an independent risk factor for atherosclerosis,[4-6] can occur when the rate of appearance of TAG (R_a TAG) into the circulation exceeds rate of disappearance or disposal (R_d TAG) from the circulation. Another example is NAFLD, which occurs due to R_a into exceeding R_d from the compartment (i.e., liver in this case) of TAG over time. This increase in TAG pool size in plasma or in the liver must occur as the direct result of R_a exceeding R_d of TAG, regardless of their absolute rates, with countless permutations of the 2 processes. On the other hand, the TAG pool will remain constant if there is a close match between R_a and R_d, again regardless of their absolute rates. Thus, a physiological steady state does not mean "zero" turnover of TAG, but rather a balance between rates of appearance and disappearance. These rates cannot be captured by techniques such as various "omics" and molecular biology tools, but by stable isotope tracer techniques. While elucidation at the levels of omics as well as signaling pathways implicated in the lipid kinetics may provide valuable information, it is limited to "snap-shot" information. It has been often demonstrated that static information does not equate with actual flux rates *in vivo*.[7-10] In this regard, stable isotope tracer methodology can provide information on lipid dynamics ("kinetics"), complementary to the static information. In this review, we will discuss the dynamic nature of lipid metabolism with an emphasis on the regulation of lipid kinetics underlying changes in tissue TAG pool size in normal and pathophysiological conditions. Then, we will discuss the basic principles of stable isotope tracer methodology that can assess *in vivo* kinetics of lipid dynamics. Finally, we will provide numerical examples on how to quantify some aspects of lipid kinetics *in vivo* using the methodology in relation to health and disease.

WHY DO WE NEED *IN VIVO* LIPID KINETICS?

To facilitate understanding of why obtaining *in vivo* kinetic information for better dissecting one's health or disease status is critical, we provide here an analogy of a water tank into and out from which water moves (i.e., water turnover). **Fig. 1** shows the volume of water in the water tank is determined by 2 factors: the rate of appearance (R_a) of water into and the rate of disappearance of water out (R_d) of the tank. The pool size will stay same if 2 rates are identical as in the case of tank A. However, the water pool size will change if there is a mismatch between R_a and R_d: increase (R_a>R_d) or decrease (R_a<R_d), which is independent of their absolute

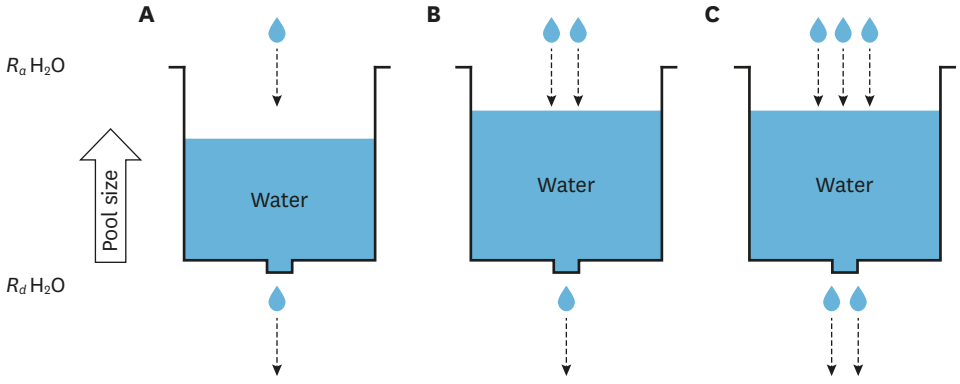

Fig. 1. The volume of water (i.e., water pool size) in the tank is determined by the balance of 2 kinetic variables: 1) rates of appearance (R_a) into and 2) disappearance (R_d) of water from the tank. The water pool size can change if an imbalance between the rates exists, regardless of their absolute rates. Furthermore, absolute rate of the water turnover may affect the quality of the water (i.e., "metabolic health").

https://doi.org/10.12997/jla.2020.9.1.110

JLA Journal of Lipid and Atherosclerosis

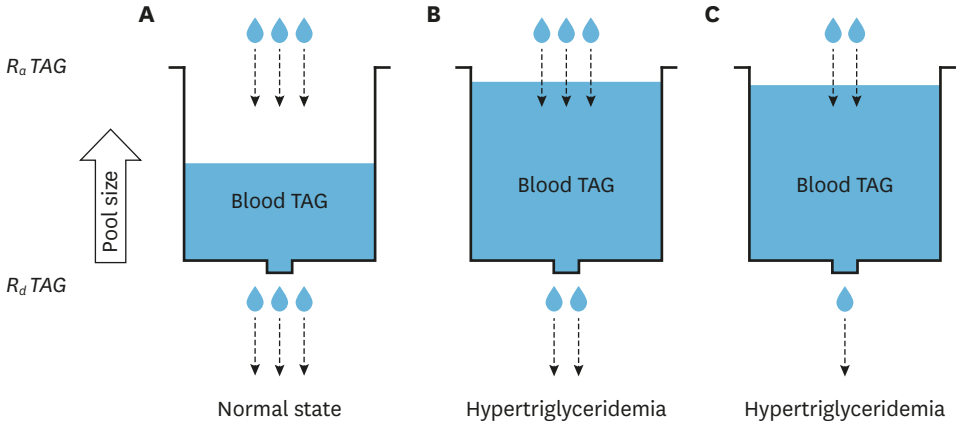

Fig. 2. TAG pool size (concentration×volume of distribution) in the tissue compartment (e.g., plasma, liver, and muscle) is determined by the balance between rates of appearance (R_a), or secretion and disappearance (R_d) or clearance of VLDL-TG (i.e., TAG turnover), regardless of their absolute rates. In tank A, the TAG pool size stays same due to the close match between R_a and R_d. However, both tanks B and C are in hypertriglyceridemic states to an identical magnitude despite different rates of each side of TAG turnover (i.e., R_a and R_d), underlying the importance of assessing dynamics of lipid metabolism in addition to the "static" snap-shot information (e.g., measurement of pool size).
TAG, triacylglycerol; VLDL-TAG, very low-density lipoprotein-triacylglycerol.

rates. To reveal the importance of the point, here we show 2 water tanks experiencing elevations in water volume at an identical rate while R_a and R_d are different between tank B and tank C in **Fig. 1**. These examples show that pool size *per se* does not provide critical information on water turnover (i.e., kinetics) and furthermore the "quality" of water, latter of which can be often influenced by the rate of water turnover (i.e., turnover replaces old with new).

The same rationale as illustrated with water kinetics applies to the assessment of the dynamics of lipid metabolism, and the limitations in relying entirely on "static" snap-shot information (e.g., measurement of pool size) to understand the regulation of lipid metabolism. For example, plasma TAG pool size is determined by the balance between R_a TAG into and R_d TAG from the tissue compartment (e.g., plasma, liver, muscle) (**Fig. 2**). As in the case of tank A, TAG pool size does not change unless there is an imbalance between R_a and R_d, as in the case of tank B and tank C. Although the rate of increase of TAG pool size in the tank B and tank C is identical, the actual rates are not same. In tank B, the mechanism responsible for the rise is not an increase in R_a TAG but a decrease in R_d. On the other hand, the cause of the rise of TAG pool size in tank C is different than tank B. In tank C, both R_a and R_d TAG are reduced compared to tank A but a decrease in R_d is much greater than that of R_a, which in turn leads to the elevation of TAG, underscoring the importance of quantifying both sides of the balance equation.

Fig. 3 shows various potential sites of dysregulation of lipids kinetics that leads to clinical phenotypes (e.g., plasma hypertriglyceridemia and NAFLD). For example, elevated plasma TAG concentrations above normal range of value (i.e., hypertriglyceridemia) must be due to the direct result of the rate of very low-density lipoprotein-triacylglycerol (VLDL-TAG) secretion (i.e., R_a) from the liver into the circulation exceeding the rate of VLDL-TAG removal (i.e., R_d) from the circulation. This imbalance can be due either to increased R_a TAG (i.e., liver VLDL-TAG secretion), decreased R_d TAG (peripheral TAG clearance via lipolysis into free fatty acid (FFA) and glycerol), or both. The site of the cause of hypertriglyceridemia will not be revealed until both sides of the balance equation (i.e., R_a and R_d TAG) are quantified.

https://doi.org/10.12997/jla.2020.9.1.110

Furthermore, even in the case when we know which side of the balance equation is the culprit of the elevated plasma TAG concentration, there are still numerous potential sites of dysregulation in the 2 rates. For example, if the problem was assumed to be due to increased R_a VLDL-TAG into the circulation, the possibility of the problem may be driven by dysregulation of intrahepatic site (i.e., dysregulation of liver metabolism *per se* such as abnormal changes at transcriptomics, proteomics, and/or signaling activity), extrahepatic site (e.g., enhanced delivery of precursor FFA to the liver via enhanced adipose tissue TAG lipolysis and subsequent R_a FFA or via *de novo* lipogenesis from carbohydrate), or both. In terms of extrahepatic origin, there are several potential sites: 1) an increased adipose tissue lipolysis, which in turn increases R_a FFA into the circulation and then to the liver, 2) a reduced intra-adipocyte cycling (re-esterification of FFA back to TAG in adipose tissue) without changes in TAG lipolysis rate, leading to increased R_a FFA, or 3) both. Changes in R_a FFA affect rate of precursor (i.e., FFA) delivery to the liver where it is largely repackaged into TAG before appearing in the plasma as VLDL-TAG. Furthermore, the rate of FFA delivery to the liver can be affected by rate of FFA uptake and subsequent metabolic processes (i.e., re-esterification to intracellular TAG or mitochondrial oxidation to CO_2) by other tissues such as skeletal muscle. Likewise, reduced R_d TAG could be due to a number of mechanisms downstream of the site of TAG removal, including reduced rates of mitochondrial fat oxidation and/or of re-esterification at the tissue (e.g., intramuscular TAG synthesis). Therefore, it is clear that in relying solely on static information without knowing dynamic nature of lipid metabolism (i.e., kinetics), it is difficult to determine the exact location(s) or "nature" of the disruption and thus to develop effective therapeutic strategies (e.g., exercise, nutrition, and drugs) and evaluate their efficacy. In the following section, we will discuss stable isotope tracer methodology that enables exploration of dynamic nature of lipid metabolism *in vivo*: basic principles of stable isotope tracer methodology in determining lipid kinetics *in vivo*.

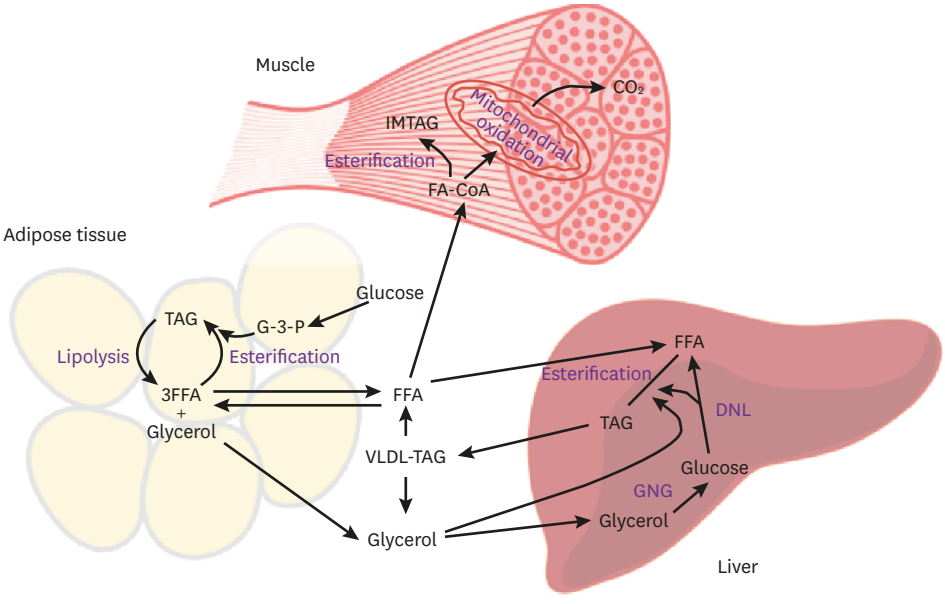

Fig. 3. Schematic of potential sites of dysregulation of lipid metabolism to which stable isotope tracers can be applied to obtaining dynamic nature of lipid kinetics.
FA-CoA, fatty acyl CoA; IMTAG, intramuscular triacylglycerol; FFA, free fatty acids; G-3-P, glycerol 3 phosphate; VLDL, very low-density lipoprotein; DNL, *de novo* lipogenesis; GNG, gluconeogenesis; TAG, triacylglycerol.

https://doi.org/10.12997/jla.2020.9.1.110

BASIC PRINCIPLES OF TRACER METHODOLOGY FOR ASSESSING LIPID KINETICS *IN VIVO*

We will focus on stable isotope tracer methodology in assessing *in vivo* metabolic flux but not radioactive isotope tracer methodology due to a number of reasons including health issues for humans. However, underlying principles of the methodologies are similar except for technical differences related to the nature of detection of the tracer. In this section, we will discuss following topics: 1) overview of performing a stable isotope tracer study in humans and 2) basic principles of stable isotope tracer methodology.

BRIEF OVERVIEW: CONDUCTING A STABLE ISOTOPE TRACER INFUSION STUDY

Fig. 4 shows a schematic overview with respect to conducting a typical stable isotope tracer infusion study to determine *in vivo* lipid kinetics in humans (also applicable to animal models). In this review, we will give a brief overview with respect to conducting a simple stable isotope tracer infusion study with which to determine some aspects of lipid kinetics *in vivo* such as R_a palmitate. Briefly, qualified subjects can take part in a study in the basal state or during or following an intervention (e.g., exercise, nutrition, and/or drugs). It is typical that an acute intervention is administered during the metabolic study (e.g., assessing flux rate at basal state and after acute exercise and/or nutritional intake). With this approach each subject essentially serves as their own control. To monitor the dynamics of the substrate

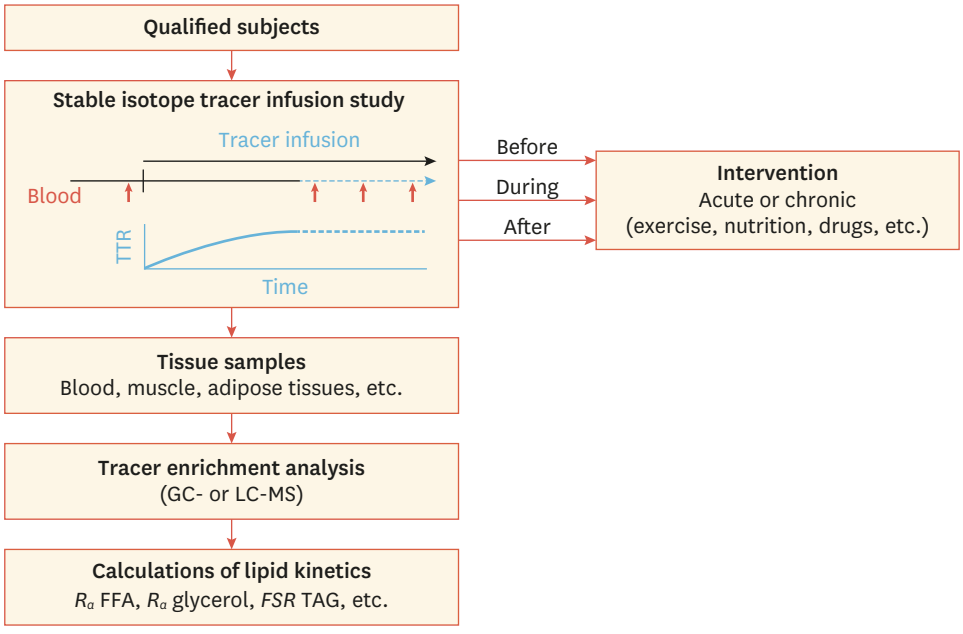

Fig. 4. Flow diagram showing the sequence of events in a stable isotope tracer infusion study for assessing metabolic kinetics such as lipids. Qualified subjects take part in tracer infusion studies before, during, and/or after an intervention. During the tracer infusion study, subjects receive a primed continuous infusion of tracer(s) at a predetermined rate (*F*) during a specified time period before and during which tissue samples (e.g., plasma) are collected for determination of enrichments by GC- or LC-MS. *In vivo* metabolic substrate kinetics (e.g., R_a FFA) are calculated based on appropriate tracer models using *F* and enrichments at steady state (E_p, dotted blue line in "stable isotope tracer infusion study"). The number of samples collected is dependent on the study design.
TTR, tracer to tracee ratio; R_a, rate of appearance; FSR, fractional synthesis rate; GC-MS, gas chromatography-mass spectrometry; LC-MS, liquid chromatography-mass spectrometry; FFA, free fatty acid; TAG, triacylglycerol.

https://doi.org/10.12997/jla.2020.9.1.110

being traced (i.e., tracee) such as FFA, one or more of tracer is administered into the body, typically intravenously. The tracer is an identical species of tracee (endogenously produced counterpart of the tracee in the body) except for differences in mass between tracer and tracee by one or more of mass units due to incorporation of one or more of heavier (stable) isotopes into the tracer molecule. The tracer is not distinguished from the tracee by the body, but the relative enrichment of the tracee by the exogenously-administered tracer is determined by mass spectrometry or appropriate analytical instruments. For example, a tracer [1-^{13}C]palmitate is one mass unit heavier than the most abundant palmitate molecule (i.e., $^{12}C_{16}{}^{1}H_{32}{}^{16}O_2$) containing only monoisotopic elements. Tracer(s) can be administered into body either as a bolus injection (then following decay of tracer enrichment relative to tracee with multiple blood samplings), a continuous infusion at a specific rate (F) with collecting a few blood samplings after achieving an isotopic plateau, at which point isotopic enrichment (E_p) does not change over time. Most commonly, a tracer is administered as a combination of a bolus injection with subsequent infusion of tracer at a specific rate (i.e., primed constant infusion). A practical advantage of a primed constant infusion of tracer is to reduce time to reach E_p and thus reduce the total experimental duration. To administer one or more of tracer(s) into the body, a catheter for intravenous infusion of tracer(s) is inserted into one hand or lower arm, while a separate catheter is placed into a vein in the other hand or lower arm for blood sampling. Blood sampling is typically from a dorsal hand vein heated at up to 60°C for about 10 minutes before sampling with a heating box or pad to "arterialize" the venous blood sample.[11] The first blood sample is collected before the tracer infusion begins in order to determine background enrichment. The background sample is used to quantify the amount of naturally-occurring tracee with the same molecular weight as the tracer. After a bolus injection of tracer, the same tracer is infused constantly at a specified rate. To determine basal substrate kinetics, blood samples (typically 3 samples) are obtained after achieving E_p. Blood samples obtained before and during the experimental period are used for determining tracer enrichment relative to tracee (i.e., tracer to tracee ratio [TTR]), typically determined using gas chromatography- or liquid chromatography-mass spectrometry (GC-MS or LC-MS). As stated above, R_a tracee is calculated as F divided by E_p. Importantly, multiple stable isotope tracers can be simultaneously administered into body for assessing various kinetics of lipids as well as other substrates such as glucose,[8,12-15] amino acids[16-20] and nitric oxide.[21-23] In this review, we will deal only with steady state substrate kinetics due to the complexity and uncertainty of non-steady state kinetics despite much of the real life being more in non-steady state. For more in-depth information regarding tracer methodology, further readings are available elsewhere.[24,25]

BASIC MODELS OF TRACER METHODOLOGY

Quantification of *in vivo* flux of lipids using tracer methodology is collectively based on 2 mathematical models: 1) tracer dilution model and 2) tracer incorporation model. In any tracer study, assessments of rate of metabolic fluxes are accomplished by using either one of these 2 or their combinations.

1. Tracer dilution model

The principle of the tracer dilution model is relatively simple as it determines the extent of dilution of tracer relative to tracee at isotopic and metabolic steady state. **Fig. 5** shows a schematic principle of how the dilution model works. Here we provide an example of *in vivo* quantification of R_a FFA in the fasted steady state. If the pool size is constant, we know that

https://doi.org/10.12997/jla.2020.9.1.110

R_a FFA is equal to R_d FFA. To determine R_a FFA, a representative tracer (i.e., palmitate tracer, denoted as red circle) is constantly infused at a fixed rate (F) intravenously into body to estimate the R_a FFA (i.e., tracee, denoted as black circle). As a function of time, relative concentration of tracer to tracee rises until it reaches plateau, which is called plateau enrichment or isotopic equilibrium (E_p). At E_p, R_a tracee palmitate is equal to R_d tracee palmitate, which is the same for R_a (i.e., F) and R_d palmitate tracer. And the ratio of these 2 (i.e., TTR or t/T) is the direct reflection of the ratio of R_a palmitate and F. In the dilution model, therefore, R_a tracee is inversely proportional to TTR for a given F. With regard to the calculation of R_a FFA, there are 2 steps: 1) R_a palmitate needs to be calculated by dividing F by E_p and then 2) R_a palmitate is then divided by the palmitate fractional contribution (FC) to total FFA to give R_a FFA. Here we provide a numerical example (**Fig. 5**). If F is 2.5 μmol/min delivered into system, and the measured E_p is 0.25, then R_a palmitate would be 10 μmol/min (i.e., F/E_p=2.5 μmol/min/0.25). If we assume the FC of palmitate to total FFA in the basal fasted state (e.g., FC=0.65),[26] then R_a FFA can be calculated to be 15.4 μmol/min (i.e., R_a palmitate/its FC=10 μmol/min/0.65=15.4 μmol/min), which is also R_d FFA, as the pool size stays same. This principle applies to the assessment of R_a of any compound (e.g., glycerol, amino acids, lactate, glucose etc.) that appears in a compartment and leaves the same compartment (e.g., plasma), to which a tracer of the same compound is introduced.

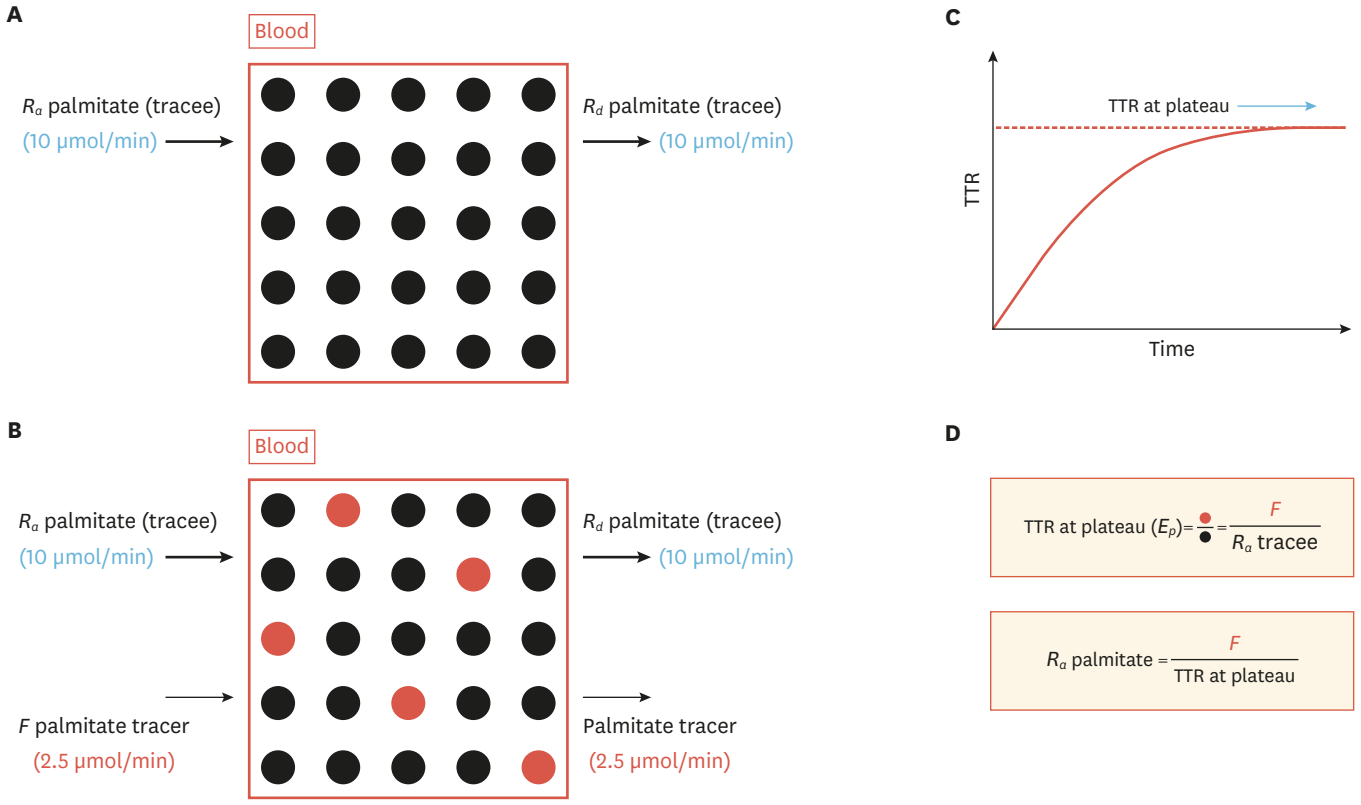

Fig. 5. Schematic principle of the tracer dilution model for assessing *in vivo* metabolic flux rate. In a steady state before introduction of tracer(s) R_a tracee (black circle) is equal to R_d tracee, both of which are unknown (A). To determine tracee kinetics, a (primed) constant infusion of tracer (e.g., palmitate, red circle) is performed during which tracer concentration relative to tracee concentration (i.e., TTR) rises to plateau where tracer infusion rate (F) is also equal to rate of tracer palmitate leaving the compartment (B). The time course of changes in isotopic enrichment after constant infusion of tracer is shown in (C). Based on these relations, it is derived that TTR at plateau is equal to ratio of F to R_a Tracee. By rearranging the equation, it is derived that R_a tracee is equal to F divided by TTR at plateau (i.e., E_p) (D).
TTR, tracer to tracee ratio.

https://doi.org/10.12997/jla.2020.9.1.110

JLA Journal of Lipid and Atherosclerosis

2. Tracer incorporation model

The principle of the tracer incorporation model is predicated on determining the rate of precursor (e.g., fatty acid, acetate unit of fatty acids, glycerol, and so on) incorporation to product (e.g., TAG). **Fig. 6** shows a schematic principle of the tracer incorporation model to determine the synthesis rate of a product. For example, TAG is comprised of fatty acids and glycerol in 3:1 stoichiometric ratio. Fatty acids comprising TAG are combinations of various fatty acid species such as palmitate (saturated fatty acid containing 16 carbons with 8 repeating acetate monomers), stearate (saturated fatty acid containing 18 carbons with 9 repeating acetate monomers), oleate (monounsaturated fatty acid containing 16 carbons with 8 repeating acetate monomers) and so on. For simplicity, here we provide an example of determining rate of synthesis of a theoretical polymer that is comprised of 2 repeating monomers (2 same units). Quantification of more complex species such as TAG (3 fatty acids+1 glycerol) and palmitate (8 repeating acetate moieties) is identical in principle.

To assess synthesis rate of TAG bound to VLDL, various tracers can be used such as fatty acid, acetate, and glycerol (backbone of TAG) (e.g., [1-^{13}C]palmitate, [U-$^{13}C_{16}$]palmitate, and [$^{2}H_{32}$]palmitate). After achieving an isotopic equilibrium of a precursor enrichment (i.e., E_p=1.0), which is far greater than what would normally be achieved (for a conceptual understanding) with a representative precursor tracer, labelled and unlabeled precursors will be incorporated into product polymers in proportional to their relative abundance. Thus, increases in product enrichment is dependent on 1) the precursor tracer enrichment achieved at isotopic equilibrium, 2) the pool size, and 3) the rate of polymer synthesis. With

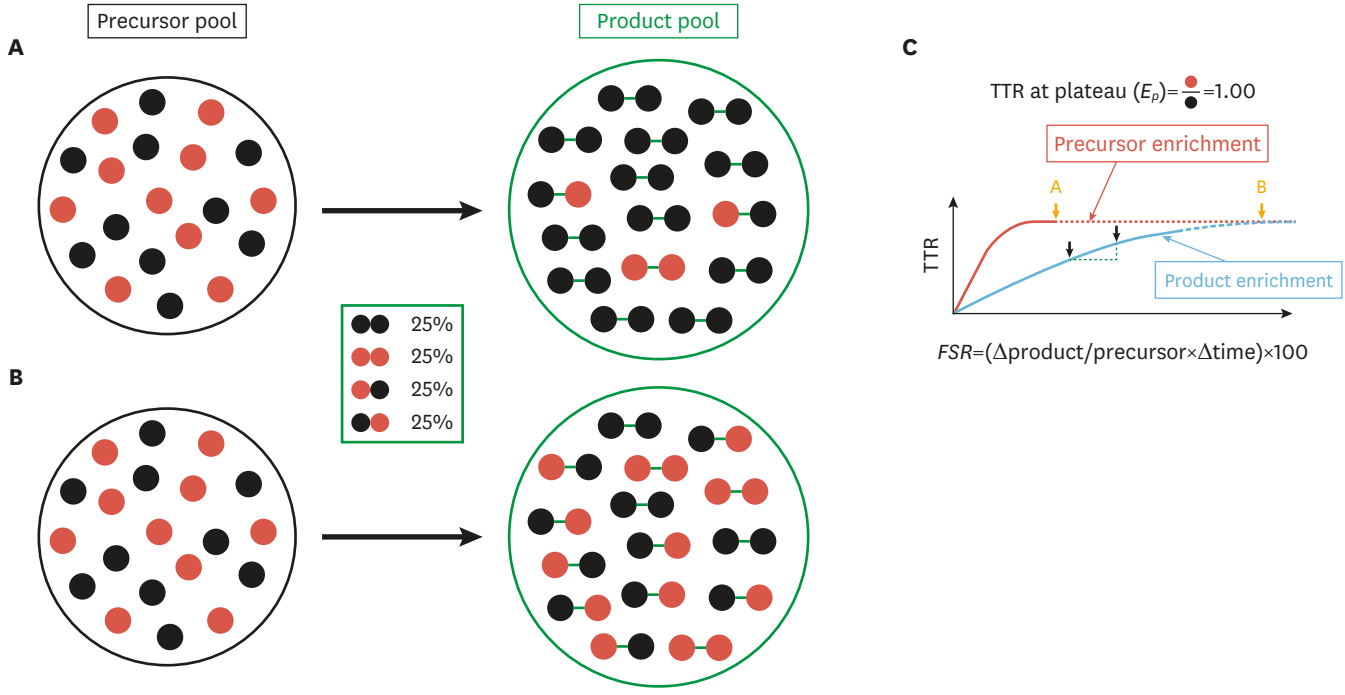

Fig. 6. Schematic principle of the tracer incorporation model of assessing *in vivo* metabolic flux rate. At an initial time period of isotopic steady state (A), both labeled and unlabeled precursors enter a synthetic pathway in proportion to their relative ratio (1:1 in this case) and enrichment of the product rises at a constant rate. However, as time goes to infinity, product enrichment ultimately reaches precursor enrichment (B). Both conditions (A, B) are described with respect to changes in enrichment of precursor and product while tissue samples are collected somewhere between these 2 (C). Fractional synthesis rate (FSR, %/time), defined as percent of pool size that has been newly synthesized for a given time, can be estimated by dividing changes in product enrichment by steady state precursor enrichment and time, multiplied by 100. To derive absolute synthesis rates, FSR needs to be multiplied by pool size. Same principle can be used for assessing synthesis of lipids such as rates of *de novo* lipogenesis and TAG synthesis.
FSR, fractional synthesis rate; TAG, triacylglycerol; TTR, tracer to tracee ratio.

https://doi.org/10.12997/jla.2020.9.1.110

an isotopic steady state of 1.0, the possible permutations of labeled compound (i.e., tracer precursor) and unlabeled compound (i.e., tracee precursor) are 4, i.e., unlabeled-unlabeled (25%), unlabeled-labeled (25%), labeled-unlabeled (25%), and labeled-labeled (25%) with the exact same probability of each case. And regardless of the turnover rate and size of the pool of the product, the product enrichment will continue to increase until it becomes equal to the precursor enrichment. Measurement of the synthesis rate of a polymer is determined as a change in product enrichment over a given time period divided by steady state precursor enrichment, multiplied by 100 (to express the rate as %/time). For example, if product enrichment was changed from 0.01 at time=0 hour (t_1) to 0.05 at time=4 hour (t_1) (thus, a change in product enrichment=0.05−0.01=0.04) with a steady state precursor enrichment of 0.10 from t_1 and t_2. Then fractional synthesis rate (FSR) of the polymer can be calculated as [0.04/(0.10×4)]×100=10%/h, which means that 10% of the pool size was newly synthesized over 1 hour. This value actually does not provide absolute synthesis rate. To obtain the absolute rate of polymer synthesis, the FSR must be multiplied by the pool size. For an example of plasma TAG with assumptions of effective volume of distribution of TAG (i.e., plasma volume) being 3 L and TAG concentration being 100 mg/dL (or 1 g/L), the pool size is 3 g of plasma TAG (i.e., 100 mg/dL×3 L=3 g). If we use the same FSR (i.e., 10%/h, shown above) and the pool size of 3 g, then absolute rate of TAG synthesis will be 300 mg TAG/h (i.e., 3 g×10%/h). **Fig. 6A** shows the principles of how the tracer incorporation model works: precursor enrichment is at isotopic equilibrium (E_p) and product is being labeled at a constant rate. As time goes, product enrichment will rise and then plateaued where enrichments of precursor and products become equal, the fractional synthetic rate can be calculated before this happens (**Fig. 6B**). **Fig. 6C** represents the time course changes in enrichments of precursor and product between 2 time points (t_1 and t_2) where tissues (e.g., plasma) are typically harvested to measure changes in product enrichment and precursor enrichments for quantification of TAG FSR. The FSR term is also used in determining various polymers such as protein (from amino acids),[14,18-20,27] glucose (from 2 trioses),[28,29] DNA (from bases),[28,30] RNA (from bases),[31,32] and so on. In the following section, we will show flux calculation of selected variables of lipid kinetics using stable isotope tracer methodology and mass spectrometry.

CALCULATIONS OF LIPID KINETICS *IN VIVO* USING STABLE ISOTOPE TRACER

In the followings, we will briefly discuss how to calculate selected *in vivo* lipid kinetics of major lipid metabolic pathways as shown in **Fig. 3** using stable isotope tracer methodology and mass spectrometry. Although not covered due to the space limitation and the intent of the review, assessments of other lipids such as cholesterol rely on the same principles.

1. Assessment of lipolysis

Mostly stored in adipose tissue, TAG is constantly broken down into FFA and glycerol in 3:1 stoichiometric ratio in a process of lipolysis via a series of enzymes including adipose triglyceride lipase (ATGL). Glycerol appears in the circulation at a rate in parallel with rate of lipolysis. Glycerol derived as the result of lipolysis does not participate in an esterification process in the adipose tissue. Glycerol kinase, an enzyme required to convert glycerol to glycerol phosphate, is absent from adipose tissue. Glycerol phosphate is the activated form of glycerol that forms the backbone of TAG and is thus essential for re-esterification. Thus, R_a glycerol reflects lipolysis and is the best proxy for lipolysis.[25,33,34] To determine R_a glycerol, a glycerol tracer (e.g., [1,1,2,3,3-$^2H_5$]glycerol) is primed constantly infused intravenously

https://doi.org/10.12997/jla.2020.9.1.110

(e.g., prime, 1 μmol/kg and *F*, 0.08 μmol/kg/min). Blood samples are collected before the tracer infusion for determining background enrichment and after achieving E_p. Enrichment is typically determined with use of GC-MS or LC-MS. If we assumed E_p to be 0.05, R_a glycerol is calculated to be 1.6 μmol/kg/min as the result of *F* divided by E_p (0.08 μmol/kg/min÷0.05=1.6 μmol/kg/min). In a steady state, R_a glycerol is equal to R_d glycerol (i.e., 1.6 μmol/kg/min).

2. Assessment of R_a FFA

FFA that are released as a result of lipolysis can either appear in the circulation at a varying rate, called R_a FFA, or may be re-esterified back to TAG by combining with glycerol phosphate. Thus, while R_a FFA is related to the rate of lipolysis, it is not a quantitative reflection of lipolysis. To assess R_a FFA, a representative tracer (e.g., [1-^{13}C]palmitate, labeled with carbon 13 at 1 carbon position) can be infused intravenously into the circulation at a constant rate, *F* (e.g., 0.04 μmol/kg/min). Blood samples are collected before the tracer infusion and after achieving E_p. A priming is not required to reach an equilibrium with a palmitate tracer due to its fast turnover rate.[35] If we assume E_p to be 0.04, R_a palmitate is then calculated by dividing *F* by E_p: 0.04 μmol/kg/min÷0.04=1 μmol/kg/min. Palmitate is not the only source of fatty acid but one species among many fatty acids. Thus, to account for contribution from other fatty acid species, R_a palmitate can be divided by its FC (assumed to be 0.65 or 65%) to estimate R_a FFA. Thus, R_a FFA can be calculated to be 1.54 μmol/kg/min as the result of R_a palmitate of 1 μmol/kg/min divided by its FC of 0.65.

3. Assessment of FFA oxidation rate

FFA that has appeared in the circulation can either be taken up by tissues such as muscle, where it is completely oxidized into CO_2 in the process of mitochondrial oxidation, or re-esterified into TAG in tissues other than adipose tissue mostly in liver, called extracellular cycling. Determination of the FFA oxidation rate is based on the incorporation of carbon from FFA to CO_2. To trace CO_2 formation derived from oxidation of FFA and thus quantify the rate of FFA oxidation, carbon-13 labeled fatty acid tracer (e.g., [1-^{13}C]palmitate) can be used with which R_a palmitate (and ultimately R_a FFA) can be simultaneously determined as shown above. For example, [1-^{13}C]palmitate can be intravenously infused at a constant rate (e.g., *F*, 0.04 μmol/kg/min). In order to estimate the FFA oxidation rate, 4 distinct values must be determined: 1) R_d FFA (=R_a FFA in a steady state), 2) carbon dioxide production rate (VCO_2/kg/min), determined via indirect calorimetry, 3) breath CO_2 enrichment (i.e., ratio of $^{13}CO_2$ of $^{12}CO_2$), determined by isotope ratio mass spectrometry, 4) % of FFA uptake that enters mitochondrial oxidation, determined as ratio of $^{13}CO_2$ excretion rate (VCO_2×breath CO_2 enrichment) to infusion rate of ^{13}C unit of palmitate tracer. In addition, account must be taken of the fraction of the carbon label that is lost via isotopic exchange in the TCA cycle. For simplicity, however, we assumed that $^{13}CO_2$ produced from the labeled palmitate as the result of mitochondrial oxidation is completely recovered in the breath, and thus the recovery correction factor (CF) is 1. The equation for estimating rate of FFA oxidation is as follows: (% of FFA uptake oxidized×R_d FFA)÷CF. Using the following data, we will show how to calculate FFA oxidation rate: 1) R_d FFA of 1.54 μmol/kg/min, 2) $^{13}CO_2$ enrichment of 0.0002, 3) VCO_2 of 100 μmol/kg/min, 4) *F* of ^{13}C unit from [1-^{13}C]palmitate of 0.04 μmol/kg/min, and 5) CF of 1 (full recovery). Then, rate of FFA oxidation =[(0.0002×100)÷(0.04÷1)]×1.54 μmol/kg/min=0.77 μmol/kg/min.

4. Assessment of TAG-fatty acid substrate cycling rate

TAG-fatty acid substrate cycling has 2 components: 1) intracellular cycling and 2) extracellular cycling. As stated above, FFA resulting from lipolysis in adipose tissue can either

https://doi.org/10.12997/jla.2020.9.1.110

be released into the circulation (R_a FFA) or re-esterified back to TAG, the process being called "intracellular cycling".[25,34,36] FFA that appears in the circulation (i.e., R_a FFA), on the other hand, can be either completely oxidized into CO_2 in the process of mitochondrial oxidation in tissues such as muscle or re-esterified into TAG in tissues other than adipose tissue, mostly in liver. The later process is called extracellular cycling.[25,34] These cycling rates can then be determined based on the information provided above (i.e., R_a FFA, R_a glycerol, FFA oxidation rate). Intracellular cycling rate is calculated as (3×R_a glycerol)−R_a FFA, later of which is predicated on the fact that 3: 1 stoichiometric relation exists between FFA and glycerol derived as the result of lipolysis. The extracellular cycling rate is calculated as R_a FFA − FFA oxidation rate, and the total cycling rate is sum of the these 2 (i.e., intracellular cycling and extracellular cycling) which is calculated as [(3×R_a glycerol)−R_a FFA]+[R_a FFA−FFA oxidation rate]=(3×R_a glycerol)−FFA oxidation rate. Using values shown above for each component, we can calculate intracellular cycling rate [(3×R_a glycerol)−R_a FFA = 3.26 μmol/kg/min], extracellular cycling rate (R_a FFA−FFA oxidation rate=0.77 μmol/kg/min), and total cycling rate [(3×R_a glycerol)−FFA oxidation rate=4.03 μmol/kg/min].

5. Assessment of VLDL-TAG synthesis rate

VLDL-TAG synthesis is a large fraction of the extracellular recycling, regulation of which is implicated in clinical conditions such as cardiovascular events.[37,38] The first step in determining the VLDL-TAG synthesis rate (and subsequent VLDL-TAG secretion rate) is to determine VLDL-TAG FSR. Several tracers can be used for assessing FSR of VLDL-TAG, including palmitate,[39] acetate,[40] glycerol[34] and even deuterium oxide.[41] Here we will discuss the calculation of VLDL-TG FSR again using [1-^{13}C]palmitate. As stated above, FSR is calculated as changes in product enrichment divided by precursor enrichment and time, multiplied by 100 (to express it as %/time).[24] For example, if plasma palmitate enrichment achieved at isotopic steady state (i.e., E_p) is 0.04 above background, and changes in enrichment of palmitate derived from plasma VLDL-TAG (i.e., product enrichment) elapsed over an experimental time period (e.g., 3 hours) is 0.03, then VLDL-TAG FSR is calculated to be 0.03÷(0.04×3 hours)=0.25/h (or 25%/h). This means that 25% of plasma VLDL-TAG pool is newly synthesized per hour. To obtain an absolute synthesis rate of VLDL-TAG, FSR (i.e., 0.25) needs to be multiplied by the pool size (VLDL-TAG concentrations x volume of distribution). If the TAG concentration is assumed to be 100 mg/dL and the volume of distribution of VLDL-TAG is 3 L, then calculation of absolute VLDL-TAG synthesis rate is as follows: 0.25/h×100 mg/dL×3 L=750 mg/h.

OTHER CONSIDERATIONS AND LIMITATIONS

Despite the beauty of assessing *in vivo* dynamics with stable isotope tracer methodology, some considerations or limitations are worth to mention. First, stable isotope tracer methodology in human study is largely limited to the assessments of *in vivo* kinetics at whole body level (but not at tissue or organ levels) as tissues other than blood, such as often muscle and adipose tissue, is usually not available. Thus, assessment of tissue specific kinetics is typically limited unless invasive catheterizations for arteriovenous balance technique and tissue biopsy are available with an accurate assessment of tissue/organ blood flow measurement.[25] Second, the use of tracer methodology requires a number of assumptions to be satisfied to guarantee the accuracy of the kinetics. For example, it is generally assumed and valid that body cannot distinguish between tracer and tracee (called "indistinguishability"), which enables accurate tracing of the movement of the tracee.[25,42]

https://doi.org/10.12997/jla.2020.9.1.110

Although such discrimination (i.e., isotope effect) has been reported, particularly in case of using isotope tracers labeled with heavier hydrogen such as deuterium, the reported isotope effects were due largely or entirely to tracer contamination or mathematical modeling errors.[25] For other assumptions which vary dependent on specific tracer models employed, readers need to consult with the more comprehensive reference.[25,42]

SUMMARY AND CONCLUSIONS

Lipids such as TAG, fatty acids, and cholesterol are not in a static state, but in a dynamic state of constant turnover with varying rates depending on a variety of factors including physiological status, species of lipids, and the particular pool of interest. The turnover of lipids enables the maintenance of a dynamic homeostasis. Dysregulation of lipid turnover can lead to clinical conditions such as dyslipidemia, NAFLD, obesity, and related clinical conditions. The significance of "static" measurements obtained by means of molecular and "omics" tools are better understood in the context of the dynamic turnover of the lipid pools. The development and testing of the efficacy of therapeutic approaches (e.g., exercise, nutrition, and/or drugs) is best accomplished by quantification of the dynamics of lipid metabolism in health and disease.

REFERENCES

1. Schoenheimer R. The dynamic state of body constituents. Cambridge (MA): Harvard University Express; 1946.
2. Schoenheimer R, Rittenberg D. Deuterium as an indicator in the study of intermediary metabolism: VI. Synthesis and destruction of fatty acids in the organism. J Biol Chem 1937;114:381-396.
3. Rittenberg D, Schoenheimer R. Deuterium as an indicator in the study of intermediary metabolism: XI. Further studies on the biological uptake of deuterium into organic substances, with special reference to fat and cholesterol formation. J Biol Chem 1937;121:235-253.
4. Kim IY, Park S, Trombold JR, Coyle EF. Effects of moderate- and intermittent low-intensity exercise on postprandial lipemia. Med Sci Sports Exerc 2014;46:1882-1890.
PUBMED | CROSSREF
5. Kim IY, Park S, Chou TH, Trombold JR, Coyle EF. Prolonged sitting negatively affects the postprandial plasma triglyceride-lowering effect of acute exercise. Am J Physiol Endocrinol Metab 2016;311:E891-E898.
PUBMED | CROSSREF
6. Bansal S, Buring JE, Rifai N, Mora S, Sacks FM, Ridker PM. Fasting compared with nonfasting triglycerides and risk of cardiovascular events in women. JAMA 2007;298:309-316.
PUBMED | CROSSREF
7. Bukhari SS, Phillips BE, Wilkinson DJ, Limb MC, Rankin D, Mitchell WK, et al. Intake of low-dose leucine-rich essential amino acids stimulates muscle anabolism equivalently to bolus whey protein in older women at rest and after exercise. Am J Physiol Endocrinol Metab 2015;308:E1056-E1065.
PUBMED | CROSSREF
8. Perry RJ, Wang Y, Cline GW, Rabin-Court A, Song JD, Dufour S, et al. Leptin mediates a glucose-fatty acid cycle to maintain glucose homeostasis in starvation. Cell 2018;172:234-248.e17.
PUBMED | CROSSREF
9. Neinast MD, Jang C, Hui S, Murashige DS, Chu Q, Morscher RJ, et al. Quantitative analysis of the whole-body metabolic fate of branched-chain amino acids. Cell Metab 2019;29:417-429.e4.
PUBMED | CROSSREF
10. Hellerstein MK. *In vivo* measurement of fluxes through metabolic pathways: the missing link in functional genomics and pharmaceutical research. Annu Rev Nutr 2003;23:379-402.
PUBMED | CROSSREF
11. McGuire EA, Helderman JH, Tobin JD, Andres R, Berman M. Effects of arterial versus venous sampling on analysis of glucose kinetics in man. J Appl Physiol 1976;41:565-573.
PUBMED | CROSSREF

12. Goodpaster BH, Wolfe RR, Kelley DE. Effects of obesity on substrate utilization during exercise. Obes Res 2002;10:575-584.
PUBMED | CROSSREF
13. Kim IY, Williams RH, Schutzler SE, Lasley CJ, Bodenner DL, Wolfe RR, et al. Acute lysine supplementation does not improve hepatic or peripheral insulin sensitivity in older, overweight individuals. Nutr Metab (Lond) 2014;11:49.
PUBMED | CROSSREF
14. Kim IY, Schutzler SE, Azhar G, Wolfe RR, Ferrando AA, Coker RH. Short term elevation in dietary protein intake does not worsen insulin resistance or lipids in older adults with metabolic syndrome: a randomized-controlled trial. BMC Nutr 2017;3:33.
PUBMED | CROSSREF
15. Chopra S, Rathore A, Younas H, Pham LV, Gu C, Beselman A, et al. Obstructive sleep apnea dynamically increases nocturnal plasma free fatty acids, glucose, and cortisol during sleep. J Clin Endocrinol Metab 2017;102:3172-3181.
PUBMED | CROSSREF
16. Gjedsted J, Buhl M, Nielsen S, Schmitz O, Vestergaard ET, Tønnesen E, et al. Effects of adrenaline on lactate, glucose, lipid and protein metabolism in the placebo controlled bilaterally perfused human leg. Acta Physiol (Oxf) 2011;202:641-648.
PUBMED | CROSSREF
17. Kim IY, Shin YA, Schutzler SE, Azhar G, Wolfe RR, Ferrando AA. Quality of meal protein determines anabolic response in older adults. Clin Nutr 2018;37:2076-2083.
PUBMED | CROSSREF
18. Kim IY, Schutzler S, Schrader A, Spencer HJ, Azhar G, Ferrando AA, et al. The anabolic response to a meal containing different amounts of protein is not limited by the maximal stimulation of protein synthesis in healthy young adults. Am J Physiol Endocrinol Metab 2016;310:E73-E80.
PUBMED | CROSSREF
19. Kim IY, Park S, Smeets ET, Schutzler S, Azhar G, Wei JY, et al. Consumption of a specially-formulated mixture of essential amino acids promotes gain in whole-body protein to a greater extent than a complete meal replacement in older women with heart failure. Nutrients 2019;11:E1360.
PUBMED | CROSSREF
20. Kim IY, Schutzler S, Schrader A, Spencer H, Kortebein P, Deutz NE, et al. Quantity of dietary protein intake, but not pattern of intake, affects net protein balance primarily through differences in protein synthesis in older adults. Am J Physiol Endocrinol Metab 2015;308:E21-E28.
PUBMED | CROSSREF
21. de Betue CT, Joosten KF, Deutz NE, Vreugdenhil AC, van Waardenburg DA. Arginine appearance and nitric oxide synthesis in critically ill infants can be increased with a protein-energy-enriched enteral formula. Am J Clin Nutr 2013;98:907-916.
PUBMED | CROSSREF
22. Castillo L, Beaumier L, Ajami AM, Young VR. Whole body nitric oxide synthesis in healthy men determined from [15N] arginine-to-[15N]citrulline labeling. Proc Natl Acad Sci U S A 1996;93:11460-11465.
PUBMED | CROSSREF
23. Kim IY, Schutzler SE, Schrader A, Spencer HJ, Azhar G, Deutz NE, et al. Acute ingestion of citrulline stimulates nitric oxide synthesis but does not increase blood flow in healthy young and older adults with heart failure. Am J Physiol Endocrinol Metab 2015;309:E915-E924.
PUBMED | CROSSREF
24. Kim IY, Suh SH, Lee IK, Wolfe RR. Applications of stable, nonradioactive isotope tracers in *in vivo* human metabolic research. Exp Mol Med 2016;48:e203.
PUBMED | CROSSREF
25. Wolfe RR, Chinkes DL. Isotope tracers in metabolic research: principles and practice of kinetic analysis. New York (NY): Wiley-Liss; 2004.
26. Mazzeo RS, Brooks GA, Schoeller DA, Budinger TF. Disposal of blood [1-13C]lactate in humans during rest and exercise. J Appl Physiol (1985) 1986;60:232-241.
PUBMED | CROSSREF
27. Kim IY, Schutzler S, Schrader AM, Spencer HJ, Azhar G, Wolfe RR, et al. Protein intake distribution pattern does not affect anabolic response, lean body mass, muscle strength or function over 8 weeks in older adults: a randomized-controlled trial. Clin Nutr 2018;37:488-493.
PUBMED | CROSSREF
28. Martini WZ, Chinkes DL, Wolfe RR. Quantification of DNA synthesis from different pathways in cultured human fibroblasts and myocytes. Metabolism 2004;53:128-133.
PUBMED | CROSSREF

29. Fulks RM, Li JB, Goldberg AL. Effects of insulin, glucose, and amino acids on protein turnover in rat diaphragm. J Biol Chem 1975;250:290-298.
PUBMED

30. Zhang XJ, Chinkes DL, Wu Z, Martini WZ, Wolfe RR. Fractional synthesis rates of DNA and protein in rabbit skin are not correlated. J Nutr 2004;134:2401-2406.
PUBMED | CROSSREF

31. Brook MS, Wilkinson DJ, Mitchell WK, Lund JL, Phillips BE, Szewczyk NJ, et al. A novel D_2O tracer method to quantify RNA turnover as a biomarker of *de novo* ribosomal biogenesis, *in vitro*, in animal models, and in human skeletal muscle. Am J Physiol Endocrinol Metab 2017;313:E681-E689.
CROSSREF

32. Khairallah EA, Mortimore GE. Assessment of protein turnover in perfused rat liver. Evidence for amino acid compartmentation from differential labeling of free and tRNA-gound valine. J Biol Chem 1976;251:1375-1384.
PUBMED

33. Wolfe RR, Peters EJ, Klein S, Holland OB, Rosenblatt J, Gary H Jr. Effect of short-term fasting on lipolytic responsiveness in normal and obese human subjects. Am J Physiol 1987;252:E189-E196.
PUBMED

34. Wolfe RR, Peters EJ. Lipolytic response to glucose infusion in human subjects. Am J Physiol 1987;252:E218-E223.
PUBMED

35. Greenough WB 3rd, Crespin SR, Steinberg D. Infusion of long-chain fatty acid anions by continuous-flow centrifugation. J Clin Invest 1969;48:1923-1933.
PUBMED | CROSSREF

36. Hellerstein MK, Benowitz NL, Neese RA, Schwartz JM, Hoh R, Jacob P 3rd, et al. Effects of cigarette smoking and its cessation on lipid metabolism and energy expenditure in heavy smokers. J Clin Invest 1994;93:265-272.
PUBMED | CROSSREF

37. Fontbonne A, Eschwège E, Cambien F, Richard JL, Ducimetière P, Thibult N, et al. Hypertriglyceridaemia as a risk factor of coronary heart disease mortality in subjects with impaired glucose tolerance or diabetes. Results from the 11-year follow-up of the Paris Prospective Study. Diabetologia 1989;32:300-304.
PUBMED | CROSSREF

38. Roche HM, Gibney MJ. The impact of postprandial lipemia in accelerating atherothrombosis. J Cardiovasc Risk 2000;7:317-324.
PUBMED | CROSSREF

39. Donnelly KL, Smith CI, Schwarzenberg SJ, Jessurun J, Boldt MD, Parks EJ. Sources of fatty acids stored in liver and secreted via lipoproteins in patients with nonalcoholic fatty liver disease. J Clin Invest 2005;115:1343-1351.
PUBMED | CROSSREF

40. Sidossis LS, Coggan AR, Gastaldelli A, Wolfe RR. Pathway of free fatty acid oxidation in human subjects. Implications for tracer studies. J Clin Invest 1995;95:278-284.
PUBMED | CROSSREF

41. Turner SM, Murphy EJ, Neese RA, Antelo F, Thomas T, Agarwal A, et al. Measurement of TG synthesis and turnover in vivo by 2H2O incorporation into the glycerol moiety and application of MIDA. Am J Physiol Endocrinol Metab 2003;285:E790-E803.
PUBMED | CROSSREF

42. Cobelli C, Foster D, Toffolo G. Tracer kinetics in biomedical research. Boston (MA): Springer US; 2002.